Published in final edited form as:
Cancer Res. 2009 March 15; 69(6): 2540–2549. doi:10.1158/0008-5472.CAN-08-1547.

Epidermal Growth Factor Receptor and PTEN Modulate Tissue Factor Expression in Glioblastoma through JunD/Activator Protein-1 Transcriptional Activity

Yuan Rong[1,5], **Vladimir E. Belozerov**[2,5], **Carol Tucker-Burden**[1,5], **Gang Chen**[1,5], **Donald L. Durden**[3,4,5], **Jeffrey J. Olson**[2,5], **Erwin G. Van Meir**[2,3,5], **Nigel Mackman**[6], and **Daniel J. Brat**[1,5]

[1] Department of Pathology and Laboratory Medicine, Aflac Cancer Center and Blood Disorders Services, Atlanta, Georgia

[2] Department of Neurosurgery, Aflac Cancer Center and Blood Disorders Services, Atlanta, Georgia

[3] Department of Hematology and Medical Oncology, Aflac Cancer Center and Blood Disorders Services, Atlanta, Georgia

[4] Department of Pediatrics, Aflac Cancer Center and Blood Disorders Services, Atlanta, Georgia

[5] Winship Cancer Institute, Emory University School of Medicine, Atlanta, Georgia

[6] Department of Hematology/Oncology, University of North Carolina, Chapel Hill, North Carolina

Abstract

Hypoxia and necrosis are fundamental features of glioblastoma (GBM) and their emergence is critical for the rapid biological progression of this fatal tumor; yet, underlying mechanisms are poorly understood. We have suggested that vaso-occlusion following intravascular thrombosis could initiate or propagate hypoxia and necrosis in GBM. Tissue factor (TF), the main cellular initiator of coagulation, is overexpressed in GBMs and likely favors a thrombotic microenvironment. *Epidermal growth factor receptor* (*EGFR*) amplification and *PTEN* loss are two common genetic alterations seen in GBM but not in lower-grade astrocytomas that could be responsible for TF up-regulation. The most frequent *EGFR* mutation in GBM involves deletion of exons 2 to 7, resulting in the expression of a constitutively active receptor, EGFRvIII. Here, we show that overexpression of EGFR or EGFRvIII in human glioma cells causes increased basal TF expression and that stimulation of EGFR by its ligand, EGF, leads to a marked dose-dependent up-regulation of TF. In all cases, increased TF expression led to accelerated plasma coagulation *in vitro*. EGFR-mediated TF expression depended most strongly on activator protein-1 (AP-1) transcriptional activity and was associated with c-Jun NH_2-terminal kinase (JNK) and JunD activation. Restoration of PTEN expression in *PTEN*-deficient GBM cells diminished EGFR-induced TF expression by inhibiting JunD/AP-1 transcriptional activity. PTEN mediated this effect by antagonizing phosphatidylinositol 3-kinase activity, which in turn attenuated both Akt and JNK activities. These mechanisms are likely at work *in vivo*, as EGFR expression was highly correlated with TF expression in human high-grade astrocytoma specimens.

Requests for reprints: Daniel J. Brat, Department of Pathology and Laboratory Medicine, Emory University Hospital, G-169, 1364 Clifton Road Northeast, Atlanta, GA 30322. Phone: 404-712-1266; Fax: 404-727-3133; dbrat@emory.edu.

Note: Supplementary data for this article are available at Cancer Research Online (http://cancerres.aacrjournals.org/).

Disclosure of Potential Conflicts of Interest
No potential conflicts of interest were disclosed.

Introduction

Glioblastoma (GBM; WHO grade 4) is the most common primary brain tumor in adults and also the most malignant (1). It is distinguished pathologically from lower-grade astrocytomas (grades 2 and 3) by necrosis and microvascular hyperplasia, a florid form of angiogenesis. Although it is recognized that hypoxia associated with necrosis causes microvascular hyperplasia in the periphery of the tumor, compelling explanations for the development of hypoxia and necrosis in GBM have not been established. We have suggested that vascular pathology may initiate this cascade (2). Nearly all GBMs display microscopic evidence of intravascular thrombosis, whereas lower-grade astrocytomas rarely show this finding (3,4). Both pathologic observations and experimental evidence suggest that hypoxia and necrosis within GBMs could be initiated or propagated by vaso-occlusion secondary to intravascular thrombosis in a manner that drives tumor progression (2,4,5). The development of thrombosis may be due in part to the deregulated expression of procoagulant molecules.

One of the most highly up-regulated and potent prothrombotic factors in human cancer is tissue factor (TF), a 47-kDa transmembrane glycoprotein receptor that is a critical regulator of tissue homeostasis (6). A direct correlation between TF levels and tumor grade has been noted for multiple tumor types (7), including gliomas (8). In addition to its prothrombotic function, TF directly promotes tumor invasiveness and angiogenesis by intracellular signals through its cytoplasmic tail, and indirectly through the activation of protease-activated receptor (PAR) 1 and PAR2 (2,9).

Two common and highly specific genetic events associated with the GBM histology are *epidermal growth factor receptor* (*EGFR*) amplification and *PTEN* loss. The *EGFR* gene is amplified in 40% to 50% of GBMs and this event is often accompanied by genetic alterations (10). The most common mutant, *EGFRvIII*, is formed following the deletion of exons 2 to 7, resulting in a constitutively active transmembrane receptor that lacks a functional ligand-binding domain (11). EGFR activation causes a variety of downstream biological processes associated with tumor growth, invasion, and angiogenesis (12). *PTEN*, a tumor suppressor gene implicated in multiple human cancers, is inactivated by mutation in 20% to 40% of GBMs and lost through other mechanisms in a much larger percentage (13–15). In the current study, we investigated whether EGFR or EGFRvIII caused increased TF expression by GBM cells and explored the relationship between EGFR and PTEN signaling in this regulation. We found that EGFR strongly induced TF expression by up-regulating JunD/activator protein-1 (AP-1) transcriptional activity on the *TF* promoter and was regulated by c-Jun NH_2-terminal kinase (JNK). Reconstitution of PTEN in *PTEN*-deficient GBM cells attenuated EGFR-induced TF expression by antagonizing phosphatidylinositol 3-kinase (PI3K) activity, which in turn reduced both Akt and JNK activities. Regulation of TF expression at the AP-1 site by PTEN was primarily due to its inhibition of JunD activity. Finally, in human high-grade astrocytomas, we found that EGFR protein expression was highly correlated with TF expression by neoplastic cells.

Materials and Methods

Cell lines

The human GBM cell line U87MG was cultured in DMEM with 10% fetal bovine serum. U87MG-wt-EGFR and U87MG-EGFRvIII cell lines (kindly provided by Frank Furnari and Webster Cavenee, Ludwig Institute, San Diego, CA) were cultured in the same conditions. The lentiviral vector expressing PTEN was constructed using the FUW vector as previously described (16). The full-length COOH terminally HA-tagged human PTEN cDNA (17) was subcloned into the *Eco*RI site of FUW. The resulting PTEN-HA/FUW plasmid was used to produce lentiviral particles using ViralPower Lentiviral Expression System (Invitrogen). Both

cell lines were infected with either the PTEN-HA or green fluorescent protein (GFP) lentiviruses and propagated as stable cell lines.

Reagents and chemicals

PD158780, SP600125, LY294002, and U0126 were from EMD Biosciences, Inc.; rapamycin was from LC Laboratories; EGF was from Sigma-Aldrich; and the citrated human plasma was from Precision Biologic. Neoplastine (Diagnostica Stago) and human plasma depleted of factor VII (R2 Diagnostics) were used as positive and negative controls, respectively.

Immunohistochemistry

Archived surgically resected GBM (23 cases) and anaplastic astrocytoma (AA; 7 cases) specimens were obtained from Emory University Hospital Department of Pathology. GBMs were selected from patients with no previous radiation or chemotherapy. Paraffin-embedded sections were deparaffinized and subjected to heat-induced epitope retrieval by steaming for 15 min. For TF, slides were incubated with primary antibody (1:100; American Diagnostica) at 4°C for overnight. Avidinbiotin-peroxidase complex was used to detect the antibodies using 3,3′-diaminobenzidine (DAB) as the chromogen. For EGFR, slides were incubated with primary antibody (1:25; ZYMED Laboratories) at room temperature for 1 h and detected with goat anti-mouse IgG-alkaline phosphatase conjugate (1:100; Molecular Probes) using Fast Red (ZYMED Laboratories) as the substrate. Staining intensity of EGFR and TF in neoplastic cells was graded on a scale of 0 (no staining) to 3+ (strong staining) without knowing *EGFR* gene status or diagnosis.

Fluorescence *in situ* hybridization analysis of *EGFR* gene amplification

On the same set of histologic sections, we used the commercially available LSI EGFR SpectrumOrange/CEP 7 SpectrumGreen dual-color probe set (Vysis, Inc., Abbott Laboratories), which included directly labeled DNA fluorescence *in situ* hybridization (FISH) probes for the *EGFR* gene (SpectrumOrange) and the centromere of chromosome 7 (SpectrumGreen). Nuclei were counterstained with 4′,6-diamidino-2-phenylindole (Molecular Probes). Detection of an average of >10 *EGFR* signals per nucleus was defined as amplification and detection of <6 *EGFR* signals per nucleus was defined as nonamplified.

Protein extraction from human GBM specimens

Eleven frozen human GBM specimens (100 mg) were obtained from the brain tumor bank of the Winship Cancer Institute. Proteins were extracted using Trizol LS reagent (Invitrogen) and expression of EGFR and TF was determined by Western blot.

Plasmids and transfections

The human *TF* promoter-luciferase reporter plasmids were as described previously (18). The constructs containing mutations in each of the Egr-1 [pTF(Egr-1m)] or Sp1 sites [pTF(Sp1m)] have been reported previously (19). The AP-1 luciferase plasmid (pAP-1-Luc) and the control plasmid (pLuc-MCS) were from Stratagene. The dominant-negative mutant c-Jun expression plasmid (c-Jun^{DN}) and the control vector were provided by Micheal J. Birrer (National Cancer Institute, Bethesda, MD). The dominant-negative mutant JunD expression plasmid (JunD^{DN}) and the control vector were provided by Lester Lau (University of Illinois, Chicago, IL). Transient transfection of plasmids was carried out using Gene Porter (Gene Therapy Systems, Inc.) and performed in triplicate. The results were calculated as the activity of firefly luciferase relative to that of the *Renilla* luciferase.

RNA interference

Small interfering RNAs (siRNA) against JNK1, JNK2, c-Jun, JunD, and rhodamine-labeled nonsilencing siRNA were purchased from Qiagen. Seventy-two hours after transfection, glioma cells were harvested for Western blot analysis.

Western blot

Cells were lysed in radioimmunoprecipitation assay buffer supplemented with 1 mmol/L phenylmethylsulfonyl and the protease inhibitor cocktail (Santa Cruz Biotechnology). Lysates were clarified by centrifugation at 10,000 × *g* for 10 min at 4°C. The NE-PER Nuclear and Cytoplasmic Extraction Reagents (Pierce Biotechnology) were used to separate nuclear and cytoplasmic proteins. Equal amounts of protein were separated on a 10% SDS-PAGE and transferred to nitrocellulose membranes. Membranes were blocked with 5% nonfat dry milk for 1 h and incubated with primary antibodies in 5% bovine serum albumin overnight at 4°C. The antibodies were used against Akt, phosphorylated Akt (p-Akt; Ser^{473}), extracellular signal-regulated kinase 1/2 (ERK1/2), phosphorylated ERK1/2, PTEN, c-Jun, phosphorylated c-Jun (p-c-Jun; Ser^{73}), phosphorylated s6rp, and nuclear factor κB1 (NFκB1; Cell Signaling Technology); TF (American Diagnostica); HA. 11 (Covance); phosphorylated JNK1/2 (p-JNK1/2), JNK1/2, and JunD (ZYMED Laboratories); and JNK2, histone H1, and β-actin (Santa Cruz Biotechnology).

ELISA for interleukin-8

Interleukin-8 (IL-8) levels in serum-free medium of U87MG-EGFRvIII and U87MG-wt-EGFR cells treated with NFκB1 siRNA were measured by ELISA (R&D Systems). A complete description of the IL-8 analysis is found within Supplementary Materials and Methods.

Plasma clotting assay

Plasma clotting times induced by GBM cells were measured in triplicate using a MLA Electra 750 Coagulation Timer (Diamond Diagnostics, Inc.). Tumor cells grown in serum-free medium with or without EGF stimulation for 24 h were collected and resuspended in PBS to 1×10^6/mL. The clotting reaction was performed as previously described (6).

Statistical analysis

ANOVA was used to compare group differences. The Student's *t* test was used to assess whether differences in the values of two groups were statistically significant, with the Bonferroni correction used for multiple simultaneous comparisons. Differences were considered to be significant with $P < 0.05$. Spearman's rank test was used to evaluate the strength of correlation between EGFR and TF expression in human high-grade astrocytoma samples.

Results

wt-EGFR and EGFRvIII up-regulate TF expression in human GBM cells and cause accelerated plasma coagulation

To investigate whether wt-EGFR or EGFRvIII regulates TF expression, we used a human glioma cell line (U87MG) stably transfected to overexpress either wt-EGFR (U87MG-wt-EGFR) or EGFRvIII (U87MG-EGFRvIII). Under basal conditions, TF was strongly up-regulated by U87MG-EGFRvIII cells compared with parental U87MG or U87MG-wt-EGFR cells (Fig. 1A, *lane 3* versus *lanes 1* and *5*) based on comparison of the TF:β-actin ratios determined by densitometry. Stimulation of wt-EGFR with EGF led to its activation within 10 minutes and also caused a marked up-regulation of TF expression in a dose-dependent manner within 24 hours (Fig. 1*B*). The EGFR inhibitor PD158780 strongly attenuated EGFRvIII-

induced (Fig. 1A, *lane 4*) and partially reduced EGF-stimulated TF expression (Fig. 1A, *lane 6* versus *lane 7*), indicating that the tyrosine kinase activity of EGFR was necessary for this effect. PD158780 did not inhibit TF expression by U87MG, which expressed little, if any, EGFR protein (Fig. 1A, *lane 2*).

To determine if EGFR-induced TF was biologically active as a procoagulant at the cell surface (20), we measured the ability of glioma cell lines to induce plasma clotting *in vitro*. Neoplastine served as the positive control and consistently caused clot formation within 11 to 12 seconds. The negative control (PBS instead of tumor cells) did not cause plasma clotting within 90 seconds (data not shown). When added to plasma, cell suspensions of U87MG-EGFRvIII caused a significantly shortened plasma clotting time (19.3 ± 1.4 seconds) compared with parental U87MG (23.6 ± 0.5 seconds) and U87MG-wt-EGFR (23.8 ± 0.1 seconds; #, $P < 0.01$, one-way ANOVA and confirmed by Student's *t* test with the Bonferroni correction). When this assay was performed using human plasma lacking factor VII, the natural ligand for TF, the plasma clotting time after adding U87MG-EGFRvIII cells was significantly prolonged (> 90 seconds), strongly implicating TF-dependent mechanisms (Fig. 1*C*). Similarly, the addition of EGF to wt-EGFR glioma cells caused a dose-dependent acceleration of plasma clotting that could be reversed by the use of plasma lacking factor VII (*, $P < 0.001$, one-way ANOVA; Fig. 1*C*; data not shown). Thus, EGFRvIII-expressing gliomas show increased basal TF expression and wt-EGFR gliomas show a dose-dependent increase in TF on receptor activation. In both instances, EGFR-induced TF resulted in accelerated plasma coagulation by tumor cells *in vitro*.

AP-1 is required for both basal and EGF-stimulated TF promoter activity

To determine whether EGFR signaling augmented TF expression through transcriptional mechanisms, we examined *TF* gene promoter activity using luciferase reporter constructs. The basal human *TF* promoter (−250 to +1) consists of a distal lipopolysaccharide response element, which contains two AP-1 and one NFκB binding sites, and a more proximal serum response region, which contains three overlapping Egr-1/Sp1 binding sites (21). We used 5′-deletion constructs of the wild-type *TF* promoter [pTF(wt)] to determine which transcription factors were most relevant to basal and EGF-stimulated TF expression by EGFR (Fig. 2A, *left*). U87MG-EGFRvIII showed a greater basal *TF* promoter activity (‡, $P < 0.001$, Student's *t* test) than parental U87MG, whereas the basal promoter activity in U87MG-wt-EGFR was similar to U87MG (Fig. 2A, *right*). On EGF stimulation (50 ng/mL, 24 hours), *TF* promoter activity was significantly increased in U87MG-wt-EGFR cells and similar to levels observed in U87MG-EGFRvIII (#, $P < 0.001$). The deletion of the distal AP-1 binding sites [pTF(AP-1 del)] was associated with a markedly reduced promoter activity in all three cell lines, including the EGF-stimulated conditions [**, $P < 0.001$ versus pTF(wt)]. Further deletion of the NFκB binding site [pTF(NFκB del)] caused additional, albeit much smaller, reductions in basal *TF* promoter activity. Deletion of the promoter to −67 [pTF(vector)] resulted in the complete loss of detectable transcriptional activity, suggesting that the proximal Sp1 and Egr-1 sites are required. These data indicated that AP-1 is necessary for maximal basal and EGF-stimulated *TF* promoter activity in GBM cells.

We next examined whether EGFR-induced expression of TF might be due to activation of JNK, a critical upstream kinase that regulates AP-1 activity. EGFRvIII and EGF stimulation of wt-EGFR caused increased levels of p-JNK1 expression, but not p-JNK2, indicating specific activation of JNK1 (Fig. 2*B*). This effect was strongly attenuated by the specific JNK inhibitor SP600125, which blocks the kinase activity of JNK and results in reduced p-JNK1 levels. Both basal TF levels (EGFRvIII) and EGF-stimulated TF expression were greatly reduced by SP600125, implicating JNK1 as a necessary kinase for EGFR-induced TF expression.

The inhibitory effect of SP600125 on JNK activity was confirmed by its ability to reduce the level of its substrate, p-JunD, on Western blots (Fig. 2*C*). For these experiments, we used the p-c-JunSer^{73} antibody, which detects both p-c-Jun at Ser^{73} and p-JunD at Ser^{100}. To determine whether the solitary p-Jun band detected in Fig. 2*C* represented p-c-Jun or p-JunD, we used specific siRNA directed against c-Jun or JunD. We found that siRNA directed at JunD decreased the intensity of the p-Jun band, but siRNA directed at c-Jun did not, indicating that this band represents p-JunD (Supplementary Fig. S1*A*, *left*).

Suppression of JunD by siRNA substantially reduced EGFR-induced TF expression (Supplementary Fig. S1*A*, *right*), whereas suppression of c-Jun did not (Supplementary Fig. S1*B*, *left*), further implicating JunD in TF transcription. These findings were also supported by cotransfecting U87MG-wt-EGFR or U87MG-EGFRvIII cells with the *TF* promoter-luciferase reporter [pTF(wt)] together with either a dominant-negative mutant c-Jun (c-Jun^{DN}) or a dominant-negative mutant JunD (JunD^{DN}) expression plasmid. JunD^{DN} was capable of significantly reducing luciferase signals compared with vector controls (*, $P < 0.001$, Student's *t* test; Supplementary Fig. S1*B*, *right*), whereas expression of c-Jun^{DN} caused only a modest reduction (data not shown). We also found that knocking down JNK1 but not JNK2 by siRNA significantly reduced EGFR-induced TF expression (Fig. 2*D*; Supplementary Fig. S1*C*, *left*).

Because the *TF* promoter also contains a NFκB site that could mediate the effects of EGFR activity, we investigated the effect of its siRNA knockdown on TF expression. We found that knockdown of NFκB1 (p105/p50) did not inhibit EGFRvIII-induced or EGF-stimulated TF expression (Supplementary Fig. S1*C*, *right*). The effect of targeted siRNA against NFκB1 activity was confirmed by showing reduced expression of IL-8, a traditional target of NFκB-directed transcription (22). IL-8 levels in serum-free medium were significantly lower after silencing NFκB1 in both U87MG-EGFRvIII and U87MG-wt-EGFR (Supplementary Fig. S2). Combined, these results show that AP-1 is required for EGFR-induced TF expression and that AP-1 activity is regulated by JNK1 following EGFR stimulation. JunD is activated by JNK1 and has a major role in mediating increased AP-1 transcriptional activity.

Restoration of PTEN inhibits both basal and EGF-stimulated TF expression

PTEN loss is a genetic signature of GBM (23). To examine whether PTEN influences the EGFR-mediated expression of TF, we restored PTEN in *PTEN*-null U87MG-wt-EGFR and U87MG-EGFRvIII cells using a HA-tagged lentiviral expression vector. Infection with GFP-expressing lentivirus was used as a negative control. Restoration of *PTEN* inhibited Akt phosphorylation and also caused a marked reduction of basal TF protein expression by U87MG-EGFRvIII (Fig. 3A, *left*). It also attenuated TF expression following EGF stimulation of U87MG-wt-EGFR cells (Fig. 3A, *right*). To determine whether the effect of PTEN on TF expression was due to transcriptional activation of the *TF* gene, we performed dual-luciferase reporter assays. Lenti-PTEN-HA infection of U87MG-EGFRvIII (Fig. 3B, *left*) and U87MG-wt-EGFR (Fig. 3B, *right*) glioma cells caused a marked reduction in basal and EGF-stimulated TF promoter activity compared with lenti-GFP–transfected controls (*, $P < 0.001$ versus GFP-infected cells; #, $P < 0.001$ versus GFP-infected cells under EGF stimulation, Student's *t* test).

PTEN was recently shown to inhibit JNK through its antagonizing effect on PI3K (24). To determine the relative contribution of PI3K and JNK to the inhibition of EGFR-mediated *TF* promoter activity, we used the specific PI3K inhibitor LY294002 and the specific JNK inhibitor SP600125 in dual-luciferase assays. Both the basal (Fig. 3C, *left*) and EGF-stimulated (Fig. 3C, *right*) *TF* promoter activities were dramatically inhibited by LY294002 and SP600125, suggesting that both PI3K and JNK are important regulators of this response (*, $P < 0.001$, one-way ANOVA, confirmed by Student's *t* test with the Bonferroni correction).

PTEN antagonizes EGFR-induced AP-1 transcriptional activity

To determine if the effects of PTEN on EGFR-induced *TF* transcription were due to specific regulation of AP-1 activity, we used lenti-PTEN-HA–infected U87MG-EGFRvIII and U87MG-wt-EGFR cells with a luciferase reporter plasmid that contained AP-1 enhancer elements. PTEN substantially reduced cellular AP-1 transcriptional activity in both the basal state for EGFRvIII (*, $P < 0.005$ versus GFP-infected cells) and under EGF stimulation for wt-EGFR (#, $P < 0.005$ versus GFP-infected cells with EGF stimulation; Fig. 4*A* and *B*). We then investigated which of the Jun family member(s) of the AP-1 complex were most affected by PTEN. On Western blotting of separated nuclear and cytoplasmic proteins, we found that PTEN decreased the level of nuclear p-JNK1 and p-JunD levels in U87MG-EGFRvIII cells (Fig. 4*C*). In EGF-stimulated U87MG-wt-EGFR cells, PTEN reduced the nuclear levels of p-JNK1 and p-JunD levels but did not reduce p-c-Jun levels (Fig. 4*D*). Thus, PTEN inhibits cellular AP-1 activity mainly through down-regulation of JNK1 and JunD activities.

EGFR-induced TF expression through AP-1 activation is signaled via the PI3K and mitogen-activated protein kinase/ERK1/2 pathways

Mitogen-activated protein kinase (MAPK) and PI3K are two major downstream signaling pathways of receptor tyrosine kinases, including EGFR (25). To examine the roles of these pathways in the EGFR-mediated up-regulation of TF, we used the PI3K inhibitor LY294002, the MAPK/ERK1/2 inhibitor U0126, and the mammalian target of rapamycin (mTOR) inhibitor rapamycin. We found that LY294002 and rapamycin strongly reduced basal TF expression by U87MG-EGFRvIII and also attenuated EGF-stimulated TF in U87MG-wt-EGFR cells (Fig. 5*A* and *B*). U0126 also reduced TF expression but less potently. We also found that LY294002 reduced the levels of p-JNK1/2 in both U87MG-EGFRvIII and U87MG-wt-EGFR cells, consistent with previous reports that PI3K stimulates JNK activity (Fig. 5*C* and *D*; ref. 24). Interestingly, mTOR inhibition by rapamycin led to a moderate increase in p-JNK1/2 levels in U87MG-EGFRvIII (Fig. 5*C*), whereas it reduced p-JNK1/2 in U87MG-wt-EGFR cells under EGF stimulation (Fig. 5*D*). Mechanisms that account for this difference between EGFRvIII and wt-EGFR require further study. The increased p-JNK observed in U87MG-EGFRvIII cells following rapamycin could be due to the loss of negative feedback regulation of mTOR on EGFR, leading to enhanced JNK activity (24). p-JunD levels were greatly reduced by all three inhibitors indicating both JNK-dependent and JNK-independent regulation of JunD activity (Fig. 5*C* and *D*).

Both ERK1/2 and JNK are MAPK family members (26). Inhibition of ERK1/2 activity by U0126 did not greatly affect basal p-JNK1/2 levels in U87MG-EGFRvIII cells (Fig. 5*C*) and had moderate inhibitory effects on p-JNK1/2 in U87MG-wt-EGFR cells (Fig. 5*D*). This observation is consistent with the reports that activation of Ras/ERK1/2 directly up-regulates AP-1 transcriptional activity, whereas inhibition of ERK1/2 reduces it (27). Combined, the data suggest that EGFR-induced TF expression occurs predominantly through JNK and regulated by both PI3K and MAPK/ERK1/2.

Human GBMs overexpress EGFR and TF compared with AAs

We investigated the expression of EGFR and TF proteins in human high-grade astrocytomas, including 23 GBMs (WHO grade 4) and 7 AAs (WHO grade 3). The results of this analysis are shown in Tables 1 and 2. These specimens represent a subset of brain tumors previously investigated for the presence of intravascular thrombosis (4). Among 23 GBMs, 22 (96%) contained microscopic intravascular thrombosis as noted by the complete occlusion of vascular lumens by an organizing clot, in addition to the diagnostic features of necrosis and/or microvascular hyperplasia. None of the seven AA specimens contained intravascular thrombosis (and by definition did not contain necrosis or vascular hyperplasia). Among the GBMs, 39% (9 of 23) showed *EGFR* amplification by FISH (Fig. 6A, *left top* and *bottom*).

None of the AAs (0 of 7) showed *EGFR* amplification. In our analysis of EGFR expression by immunohistochemistry, we found that 86% (6 of 7) of AA samples showed no appreciable expression (Fig. 6A, *middle top*); in GBM specimens, 22% (5 of 23) showed strong (3+) and 35% (8 of 23) showed moderate (2+) EGFR staining (Fig. 6A, *middle bottom*; Table 1). None of the GBMs with weak (1+) or absent (0) EGFR expression showed EGFR amplification. On ANOVA analysis, GBMs as a group had significantly greater EGFR expression than AAs ($P < 0.001$). Those GBMs with *EGFR* amplification had a higher protein expression of EGFR than tumors without amplification ($P < 0.001$). Immunohistochemistry for TF in AAs showed weak (1+; 6 of 7) or absent (0; 1 of 7) staining (Fig. 6A, *right top*), whereas 30% (7 of 23) of GBMs showed strong (3+) TF expression and 39% (9 of 23) showed moderate (2+) expression (Fig. 6A, *right bottom*; Table 2). GBMs as a group showed much greater TF protein expression than AAs ($P = 0.002$). The expression of TF in *EGFR*-amplified GBMs was greater than that of nonamplified GBMs, but this difference did not achieve statistical significance on ANOVA analysis ($P = 0.22$). When all high-grade astrocytoma specimens (GBMs and AAs) were considered, there was a strong positive correlation between the expression of EGFR and TF ($\rho = 0.5$, Spearman's rank test). Thus, human GBMs show greater EGFR protein expression than AA and this is associated with both a higher expression of TF and a higher frequency of intravascular thrombosis.

To further support the above findings, proteins extracted from another 11 frozen human GBM specimens were analyzed for EGFR and TF protein expression by Western blot. The five GBMs with the strongest EGFR expression also showed the strongest TF expression (Fig. 6*B*). The six GBM specimens with the least EGFR expression showed only weak to moderate TF protein levels. EGFR:actin and TF:actin expression ratios were obtained for each specimen following densitometry of protein bands (Fig. 6*B*). Comparison of these ratios among specimens showed a strong positive correlation between EGFR and TF expression ($\rho = 0.8$, Spearman's rank test).

Discussion

Once astrocytomas have progressed to GBM, they show accelerated growth and rapid progression to death (3,28). Mechanisms responsible for the abrupt onset of explosive growth are still being defined but are likely related to the development of necrosis and angiogenesis (microvascular hyperplasia), which are two defining features of GBM histology and powerful predictors of poor prognosis (2,3,5). Necrosis and the ensuing hypoxia-induced angiogenesis could be initiated or propagated by intravascular thrombosis (2,6). Nearly all GBM specimens (grade 4) show microscopic intravascular thrombosis within tissue specimens, but lower-grade astrocytomas (grades 2 and 3) that lack necrosis only rarely do. Importantly, those grade 3 tumors that lack necrosis but show intravascular thrombosis have aggressive clinical courses, similar to GBM, suggesting that thrombosis may initiate an aggressive growth phase (4).

A strong relationship between human malignancy and abnormal blood clotting is well established but underlying mechanisms are not (3,5). One of the most highly up-regulated prothrombotic factors in human malignancy is TF, the primary cellular initiator of plasma coagulation (29,30). In astrocytomas, TF levels correlate with tumor grade and are highest in GBM. Indeed, publicly available data sets of gene expression[7] show that TF is strongly up-regulated in GBM specimens compared with lower-grade astrocytomas (31–33). Previous reports have indicated that oncogenic events could trigger TF overexpression and coagulopathy (34). In light of this, we investigated two genetic alterations specific to the GBM histology that are rare in lower-grade astrocytomas—*EGFR* amplification and rearrangement and *PTEN* loss—to define their roles in regulating TF expression (11). We found that EGFR activation was associated with marked increases in TF expression by human GBM cells, both in constitutively

[7] http://www.oncomine.org

active EGFRvIII-expressing cells and in EGF-stimulated wt-EGFR–expressing cells. In all cases, increased TF was associated with accelerated plasma coagulation dependent on the interaction of TF with factor VII.

These findings are supported by our investigations on human high-grade astrocytoma resection specimens. GBMs, which almost uniformly contain microscopic evidence of intravascular thrombosis, showed a higher frequency of *EGFR* amplification and a greater level of EGFR protein expression than AAs, and this EGFR up-regulation was strongly associated with the increased expression of TF. Thus, the expression of EGFR and TF proteins and the presence of intravascular thrombosis are tightly linked to the GBM histology. Although causality cannot be shown by our correlative analysis of human specimens, we have speculated that during the progression of astrocytomas, a prothrombotic microenvironment created by neoplastic TF expression could readily account for the presence of thrombosis in the setting of vascular leakiness.

The *TF* promoter contains multiple binding sites for transcriptional regulation, including three proximal overlapping Sp1/Egr-1 sites as well as two AP-1 and one NFκB sites located more distally. We have previously shown that Egr-1 sites are important for the hypoxic up-regulation of TF in GBM (19). Experiments using truncated mutants of the *TF* promoter in the present study indicate that the AP-1 binding site is the most critical for EGFR-induced TF up-regulation under normoxic conditions. AP-1 is not a single transcription factor but instead represents a series of related dimeric complexes of Fos and Jun family proteins that are regulated by the upstream kinase JNK1/2 (35). Our results show that JNK1 is more important than JNK2 in the regulation of AP-1 activation following EGFR stimulation but that JNK-independent mechanisms of AP-1 activity are also relevant. JNK1 activates AP-1 by phosphorylating Jun family members, including c-Jun, JunB, and JunD (36). The increased AP-1 transcriptional activity that follows EGFR stimulation is due primarily to the phosphorylation of JunD by JNK1. In support of this, the knockdown of JunD, but not c-Jun, by siRNA markedly attenuated EGFR-induced TF expression.

EGFR activation leads to a host of downstream intracellular signaling events, including activation of PI3K/Akt/mTOR (25). PI3K has been recently shown to stimulate JNK independently of Akt activation (24). Because *PTEN* loss is a frequent genetic event in GBM and its lipid phosphatase activity antagonizes the effects of PI3K (37), we explored its role in the regulation of EGFR-induced TF expression. Restoration of *PTEN* into EGFR-expressing, *PTEN*-null glioma cells caused a substantial reduction in EGFR-induced TF expression. This effect was mediated at the transcriptional level, as both p-JNK1 levels and the subsequent activation of AP-1 transcription were reduced by PTEN restoration. Importantly, we found that PTEN suppressed AP-1 activation primarily by inhibiting p-JunD, representing the first demonstration that PTEN is capable of modulating JunD/AP-1 activity in GBM cells.

In addition to JNK, the MAPK family includes ERK1/2 and p38 (38). These signaling pathways also intersect with EGFR activation and could potentially be relevant to TF up-regulation. We found that the inhibition of ERK1/2 with U0126 significantly reduced TF expression by EGFR. Similarly, the inhibition of mTOR by rapamycin reduced EGFR-induced TF expression. These inhibitors also greatly reduced p-JunD levels, suggesting a final common pathway of AP-1 transcriptional regulation.

Together, our studies provide new evidence that oncogenic mechanisms are sufficient for the up-regulation of TF expression by GBM cells, independently of hypoxia. This is an important finding as it establishes that mutation may be the first event leading to thrombosis and that the ensuing hypoxia and necrosis may amplify the effect. A prothrombotic environment caused by elevated TF could potentially lead to the emergence of necrosis, hypoxia-induced

angiogenesis, and peripheral tumor growth (5,6). Moreover, TF promotes tumor progression by intracellular signaling through its cytoplasmic tail and by activation of PARs (9,39). Our findings reinforce the need to investigate the role of TF in GBM progression *in vivo* and to define therapeutic modalities that could antagonize these mechanisms.

Supplementary Material

Refer to Web version on PubMed Central for supplementary material.

Acknowledgments

Grant support: USPHS NIH awards CA-109382 and NS053727 (D.J. Brat), CA-94233 (D.L. Durden), and CA86335 and CA116804 (E.G. Van Meir).

We thank Dr. Gabriela Denning for providing the full-length COOH terminally HA-tagged human PTEN cDNA vector, Drs. Frank Furnari and Webster Cavenee for the U87-wt-EGFR and U87-EGFRvIII cell lines, and Daniel Drake for the statistical analysis for the immunohistochemical results of human GBM specimens.

References

1. Burger PC, Green SB. Patient age, histologic features, and length of survival in patients with glioblastoma multiforme. Cancer 1987;59:1617–25. [PubMed: 3030531]
2. Rong Y, Durden DL, Van Meir EG, Brat DJ. 'Pseudo-palisading' necrosis in glioblastoma: a familiar morphologic feature that links vascular pathology, hypoxia, and angiogenesis. J Neuropathol Exp Neurol 2006;65:529–39. [PubMed: 16783163]
3. Brat DJ, Castellano-Sanchez AA, Hunter SB, et al. Pseudopalisades in glioblastoma are hypoxic, express extracellular matrix proteases, and are formed by an actively migrating cell population. Cancer Res 2004;64:920–7. [PubMed: 14871821]
4. Tehrani M, Friedman TM, Olson JJ, Brat DJ. Intravascular thrombosis in central nervous system malignancies: a potential role in astrocytoma progression to glioblastoma. Brain Pathol 2008;18:164–71. [PubMed: 18093251]
5. Brat DJ, Van Meir EG. Vaso-occlusive and prothrombotic mechanisms associated with tumor hypoxia, necrosis, and accelerated growth in glioblastoma. Lab Invest 2004;84:397–405. [PubMed: 14990981]
6. Rong Y, Post DE, Pieper RO, Durden DL, Van Meir EG, Brat DJ. PTEN and hypoxia regulate tissue factor expression and plasma coagulation by glioblastoma. Cancer Res 2005;65:1406–13. [PubMed: 15735028]
7. Contrino J, Hair G, Kreutzer DL, Rickles FR. *In situ* detection of tissue factor in vascular endothelial cells: correlation with the malignant phenotype of human breast disease. Nat Med 1996;2:209–15. [PubMed: 8574967]
8. Hamada K, Kuratsu J, Saitoh Y, Takeshima H, Nishi T, Ushio Y. Expression of tissue factor correlates with grade of malignancy in human glioma. Cancer 1996;77:1877–83. [PubMed: 8646688]
9. Belting M, Dorrell MI, Sandgren S, et al. Regulation of angiogenesis by tissue factor cytoplasmic domain signaling. Nat Med 2004;10:502–9. [PubMed: 15098027]
10. Wong AJ, Bigner SH, Bigner DD, Kinzler KW, Hamilton SR, Vogelstein B. Increased expression of the epidermal growth factor receptor gene in malignant gliomas is invariably associated with gene amplification. Proc Natl Acad Sci U S A 1987;84:6899–903. [PubMed: 3477813]
11. Nishikawa R, Ji XD, Harmon RC, et al. A mutant epidermal growth factor receptor common in human glioma confers enhanced tumorigenicity. Proc Natl Acad Sci U S A 1994;91:7727–31. [PubMed: 8052651]
12. Pore N, Jiang Z, Gupta A, Cerniglia G, Kao GD, Maity A. EGFR tyrosine kinase inhibitors decrease VEGF expression by both hypoxia-inducible factor (HIF)-1-independent and HIF-1-dependent mechanisms. Cancer Res 2006;66:3197–204. [PubMed: 16540671]
13. Duerr EM, Rollbrocker B, Hayashi Y, et al. PTEN mutations in gliomas and glioneuronal tumors. Oncogene 1998;16:2259–64. [PubMed: 9619835]

14. Li J, Yen C, Liaw D, et al. PTEN, a putative protein tyrosine phosphatase gene mutated in human brain, breast, and prostate cancer. Science 1997;275:1943–7. [PubMed: 9072974]
15. Steck PA, Pershouse MA, Jasser SA, et al. Identification of a candidate tumour suppressor gene, MMAC1, at chromosome 10q23.3 that is mutated in multiple advanced cancers. Nat Genet 1997;15:356–62. [PubMed: 9090379]
16. Lois C, Hong EJ, Pease S, Brown EJ, Baltimore D. Germline transmission and tissue-specific expression of transgenes delivered by lentiviral vectors. Science 2002;295:868–72. [PubMed: 11786607]
17. Denning G, Jean-Joseph B, Prince C, Durden DL, Vogt PK. A short N-terminal sequence of PTEN controls cytoplasmic localization and is required for suppression of cell growth. Oncogene 2007;26:3930–40. [PubMed: 17213812]
18. Bavendiek U, Libby P, Kilbride M, Reynolds R, Mackman N, Schonbeck U. Induction of tissue factor expression in human endothelial cells by CD40 ligand is mediated via activator protein 1, nuclear factor κB, and Egr-1. J Biol Chem 2002;277:25032–9. [PubMed: 11978801]
19. Rong Y, Hu F, Huang R, et al. Early growth response gene-1 regulates hypoxia-induced expression of tissue factor in glioblastoma multiforme through hypoxia-inducible factor-1-independent mechanisms. Cancer Res 2006;66:7067–74. [PubMed: 16849552]
20. Erlich J, Parry GC, Fearns C, et al. Tissue factor is required for uterine hemostasis and maintenance of the placental labyrinth during gestation. Proc Natl Acad Sci U S A 1999;96:8138–43. [PubMed: 10393961]
21. Mackman N. Regulation of the tissue factor gene. FASEB J 1995;9:883–9. [PubMed: 7615158]
22. Naugler WE, Karin M. NF-κB and cancer-identifying targets and mechanisms. Curr Opin Genet Dev 2008;18:19–26. [PubMed: 18440219]
23. Mellinghoff IK, Wang MY, Vivanco I, et al. Molecular determinants of the response of glioblastomas to EGFR kinase inhibitors. N Engl J Med 2005;353:2012–24. [PubMed: 16282176]
24. Vivanco I, Palaskas N, Tran C, et al. Identification of the JNK signaling pathway as a functional target of the tumor suppressor PTEN. Cancer Cell 2007;11:555–69. [PubMed: 17560336]
25. Vivanco I, Sawyers CL. The phosphatidylinositol 3-kinase AKT pathway in human cancer. Nat Rev Cancer 2002;2:489–501. [PubMed: 12094235]
26. Raman M, Chen W, Cobb MH. Differential regulation and properties of MAPKs. Oncogene 2007;26:3100–12. [PubMed: 17496909]
27. Feng H, Xiang H, Mao YW, et al. Human Bcl-2 activates ERK signaling pathway to regulate activating protein-1, lens epithelium-derived growth factor and downstream genes. Oncogene 2004;23:7310–21. [PubMed: 15326476]
28. Stupp R, Mason WP, van den Bent MJ, et al. Radiotherapy plus concomitant and adjuvant temozolomide for glioblastoma. N Engl J Med 2005;352:987–96. [PubMed: 15758009]
29. Rickles FR, Falanga A. Molecular basis for the relationship between thrombosis and cancer. Thromb Res 2001;102:V215–24. [PubMed: 11516455]
30. Kakkar AK, DeRuvo N, Chinswangwatanakul V, Tebbutt S, Williamson RC. Extrinsic-pathway activation in cancer with high factor VIIa and tissue factor. Lancet 1995;346:1004–5. [PubMed: 7475548]
31. Sun L, Hui AM, Su Q, et al. Neuronal and glioma-derived stem cell factor induces angiogenesis within the brain. Cancer Cell 2006;9:287–300. [PubMed: 16616334]
32. Kotliarov Y, Steed ME, Christopher N, et al. High-resolution global genomic survey of 178 gliomas reveals novel regions of copy number alteration and allelic imbalances. Cancer Res 2006;66:9428–36. [PubMed: 17018597]
33. Bredel M, Bredel C, Juric D, et al. Functional network analysis reveals extended gliomagenesis pathway maps and three novel MYC-interacting genes in human gliomas. Cancer Res 2005;65:8679–89. [PubMed: 16204036]
34. Yu JL, May L, Lhotak V, et al. Oncogenic events regulate tissue factor expression in colorectal cancer cells: implications for tumor progression and angiogenesis. Blood 2005;105:1734–41. [PubMed: 15494427]
35. Shaulian E, Karin M. AP-1 as a regulator of cell life and death. Nat Cell Biol 2002;4:E131–6. [PubMed: 11988758]

36. Antonyak MA, Kenyon LC, Godwin AK, et al. Elevated JNK activation contributes to the pathogenesis of human brain tumors. Oncogene 2002;21:5038–46. [PubMed: 12140754]

37. Luo J, Manning BD, Cantley LC. Targeting the PI3K-Akt pathway in human cancer: rationale and promise. Cancer Cell 2003;4:257–62. [PubMed: 14585353]

38. Kyriakis JM. Signaling by the germinal center kinase family of protein kinases. J Biol Chem 1999;274:5259–62. [PubMed: 10026130]

39. Palumbo JS, Talmage KE, Massari JV, et al. Tumor cell-associated tissue factor and circulating hemostatic factors cooperate to increase metastatic potential through natural killer cell-dependent and-independent mechanisms. Blood 2007;110:133–41. [PubMed: 17371949]

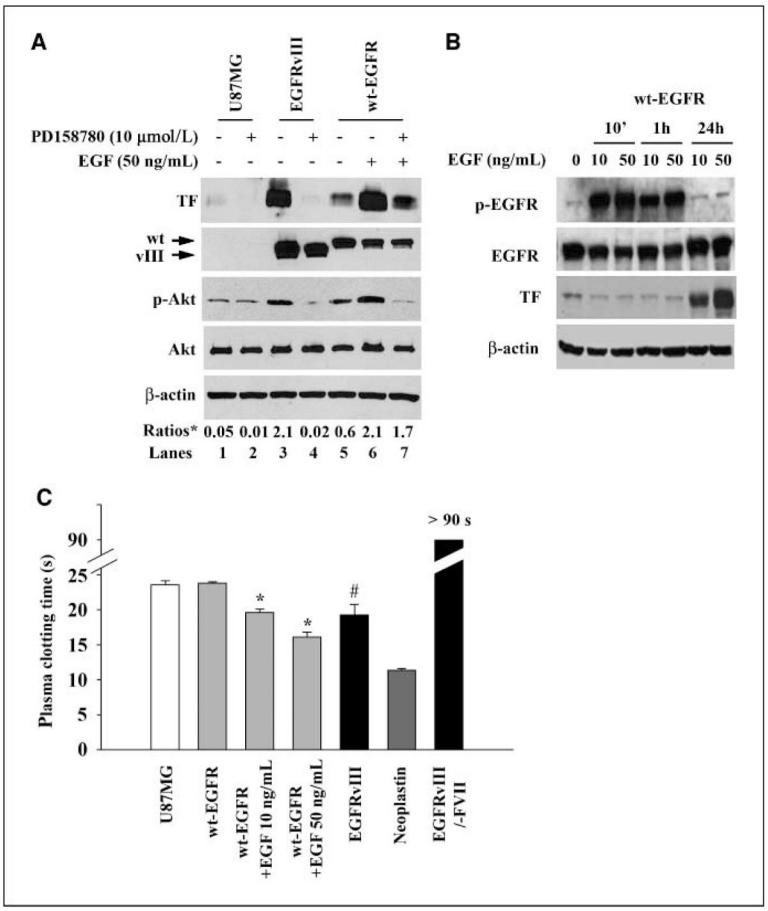

Figure 1.

wt-EGFR and EGFRvIII up-regulate TF in human GBM cells and accelerate plasma coagulation. *A*, Western blot of cell lysates from U87MG, U87MG-EGFRvIII, and U87MG-wt-EGFR cells shows higher basal TF expression by U87MG-EGFRvIII cells (*lane 3*) than U87MG (*lane 1*) and U87MG-wt-EGFR cells (*lane 5*). PD158780, a specific EGFR inhibitor, significantly reduced EGFRvIII-induced (*lane 4*) and EGF-stimulated (*lane 7* versus *lane 6*) TF expression. *Lane 2*, no inhibitory effect on TF expression was seen by U87MG cells, which showed little EGFR protein levels. Ratios (*) indicate the relative intensities of TF bands normalized to the corresponding β-actin bands. Increased p-Akt levels were observed on U87MG-EGFRvIII and EGF-stimulated U87MG-wt-EGFR cells. The effect of PD158780 on EGFR activity was confirmed by the inhibition of p-Akt levels on both cell lines. *B*, Western blot of cell lysates from U87MG-wt-EGFR cells following stimulation with EGF (10 or 50 ng/mL). Receptor activation (*p-EGFR*) was noted within 10 min. A dose-dependent up-regulation of TF expression was noted within 24 h. Total EGFR levels were not changed on EGF stimulation. *C*, the addition of U87MG-EGFRvIII glioma cells to human plasma caused a significantly shortened clotting time (19.3 ± 1.42 s) compared with U87MG (23.6 ± 0.53 s) and U87MG-wt-EGFR (23.8 ± 0.15 s). #, $P < 0.01$. No significant difference was noted in clotting times with U87MG and U87MG-wt-EGFR. Using plasma lacking factor VII (*FVII*), the clotting time after adding U87MG-EGFRvIII cells was significantly prolonged (*broken black column*, >90 s). Neoplastine was used as the positive control and consistently caused plasma clotting in 11 to 12 s. Stimulation of U87MG-wt-EGFR cells with EGF at 10 or 50 ng/mL for 24 h caused a significant and dose-dependent acceleration of plasma clotting. *, $P <$ 0.001 versus non-EGF treated.

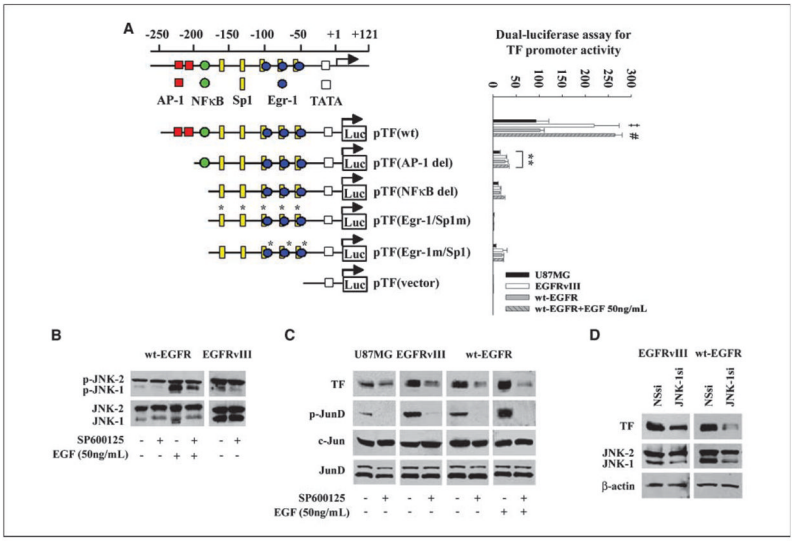

Figure 2.

AP-1 is required for both basal and EGF-stimulated *TF* promoter activity. *A, left*, schematic of human *TF* promoter and luciferase constructs. *pTF(wt)*, wild-type *TF* promoter; *pTF(AP-1 del)*, 5′-deletion of AP-1 binding sites (*red boxes*); *pTF(NFκB del)*, 5′-deletion of NFκB (*green circle*) binding sites; *pTF(Egr-1/Sp1m)*, Sp1 binding sites (*yellow bars*) are mutated; *pTF (Egr-1m/Sp1)*, Egr-1 binding sites (*blue circles*) are mutated; *pTF(vector)*, 5′-deletion of all the transcriptional binding sites. *Right*, U87MG-EGFRvIII showed higher basal *TF* promoter activity compared with U87MG and U87MG-wt-EGFR by dual-luciferase assay. ‡, $P < 0.001$. On EGF stimulation (50 ng/mL, 24 h), *TF* promoter activity was significantly increased in U87MG-wt-EGFR cells. #, $P < 0.001$ versus non–EGF-treated wt-EGFR cells. 5′-Deletion of the AP-1 binding sites from the wild-type promoter reduced promoter activity in all three cell lines under both basal and EGF-stimulated conditions. **, $P < 0.001$ versus pTF(wt). Deletion of NFκB binding sites [pTF(Egr-1/Sp1)] caused additional, but smaller, reduction in basal *TF* promoter activity. Further mutation of Sp1 binding sites or deletion of all the transcriptional binding sites resulted in the complete loss of detectable *TF* promoter activity. *B*, Western blot of cell lysates of U87MG-wt-EGFR shows increased levels of p-JNK1, but not p-JNK2, following EGF stimulation. This effect was attenuated by SP600125, a specific JNK inhibitor. Total JNK levels were not affected by SP600125. *C*, Western blot of cell lysates from U87MG, U87MG-EGFRvIII, and U87MG-wt-EGFR shows that basal levels and EGF-stimulated TF expression are greatly reduced by SP600125. The inhibitory effect of SP600125 on JNK1 activity was confirmed by its ability to reduce p-JunD levels. Total levels of JunD and c-Jun were not affected by SP600125. *D*, Western blot of cell lysates from U87MG-EGFRvIII and U87MG-wt-EGFR cells following transfection with JNK1 siRNA for 72 h. siRNA knockdown of JNK1 significantly inhibited EGFRvIII-induced and EGF-stimulated (*wt-EGFR*) TF expression. *β-actin*, loading control.

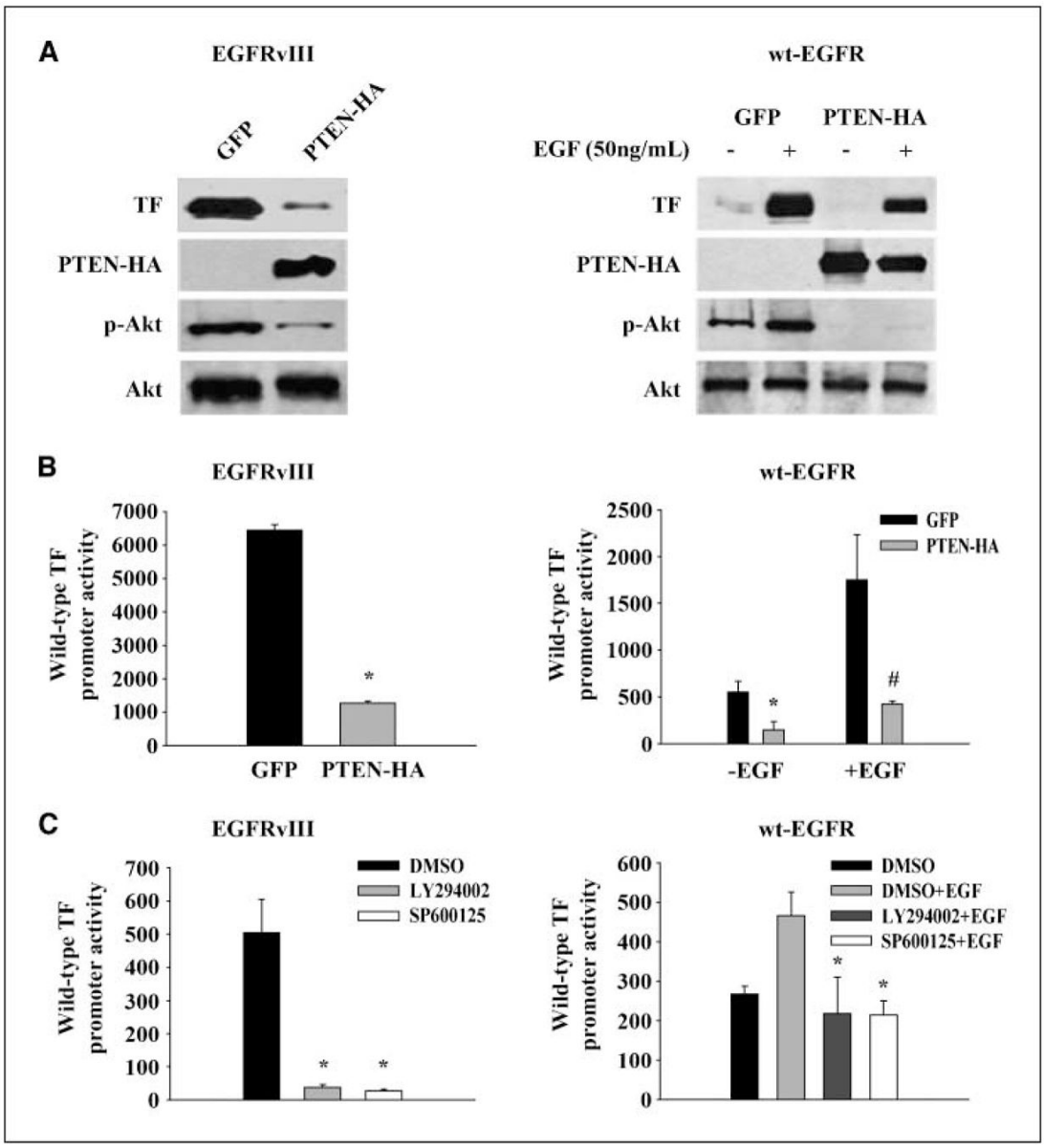

Figure 3.

Restoration of PTEN attenuates EGFR-induced TF expression. *A, left*, Western blot of U87MG-EGFRvIII cell lysates following lentiviral infection of PTEN-HA or GFP shows reduced expression of TF in PTEN-HA–infected cells; *right*, Western blot of cell lysates from U87MG-wt-EGFR cells following lentiviral infection of PTEN-HA or GFP shows reduced TF expression under both basal and EGF-stimulated (50 ng/mL, 24 h) conditions. *B, left*, dual-luciferase assay of wild-type *TF* promoter [pTF(wt)] activity in U87MG-EGFRvIII cells shows that lentiviral infection of PTEN-HA reduces promoter activity compared with GFP-infected cells. *, $P < 0.001$. *Right*, dual-luciferase assay of wild-type *TF* promoter [pTF(wt)] activity in U87MG-wt-EGFR cells infected with lenti-PTEN-HA shows reduced *TF* promoter activity under both basal (*, $P < 0.001$) and EGF-stimulated (#, $P < 0.001$) conditions compared with GFP-infected cells. *C, left*, dual-luciferase assay of wild-type *TF* promoter [pTF(wt)] activity in U87MG-EGFRvIII cells shows that inhibitors of PI3K (LY294002, 10 μmol/L) and/or JNK (SP600125, 10 μmol/L) significantly reduce *TF* promoter activity compared with the controls

(DMSO treated). *, $P < 0.001$. *Right*, dual-luciferase assay of wild-type *TF* promoter [pTF (wt)] activity in U87MG-wt-EGFR cells shows that inhibition of PI3K (LY294002, 10 μmol/L) and/or JNK (SP600125, 10 μmol/L) activity significantly reduced *TF* promoter activity in EGF-stimulated cells (50 ng/mL) compared with the control [DMSO + EGF (50 ng/mL) treated]. *, $P < 0.005$.

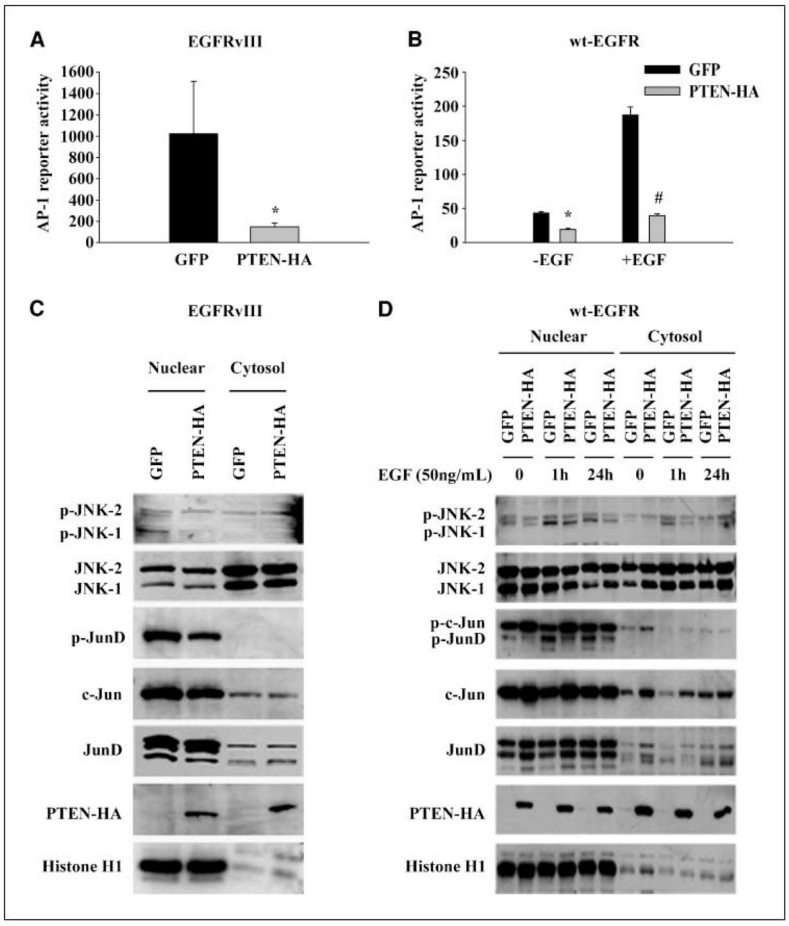

Figure 4.

PTEN antagonizes EGFR-induced TF expression by down-regulating AP-1 activity. *A*, dual-luciferase assay of AP-1 activity in U87MG-EGFRvIII cells shows that lentiviral infection of PTEN-HA causes a significant reduction of reporter activity compared with GFP-infected cells. *, $P < 0.005$. *B*, dual-luciferase assay of AP-1 activity in U87MG-wt-EGFR cells shows that lentiviral infection of PTEN-HA reduces reporter activity under basal and EGF-stimulated conditions compared with GFP-infected cells. *, $P < 0.005$ versus GFP-infected cells; #, $P < 0.001$ versus EGF-stimulated (50 ng/mL) GFP cells. *C*, Western blot of nuclear and cytoplasmic compartments of U87MG-EGFRvIII cells infected with PTEN-HA or GFP reveals a reduced expression of nuclear p-JNK1 and p-JunD levels in PTEN-HA–infected cells compared with GFP-infected cells. No differences were noted in the expression of total JNK1/2, c-Jun, or JunD. *Histone H1*, loading control for nuclear protein. *D*, Western blot of nuclear and cytoplasmic compartments of U87MG-wt-EGFR cells infected with PTEN-HA or GFP under basal (0 h) or EGF-stimulated conditions (50 ng/mL, 1 and 24 h) shows decreased expression of nuclear p-JNK1 and p-JunD levels in PTEN-HA–infected cells compared with GFP-infected cells following EGF stimulation. Total JNK, c-Jun, and JunD levels were not affected by EGF. *Histone H1*, loading controls for nuclear protein.

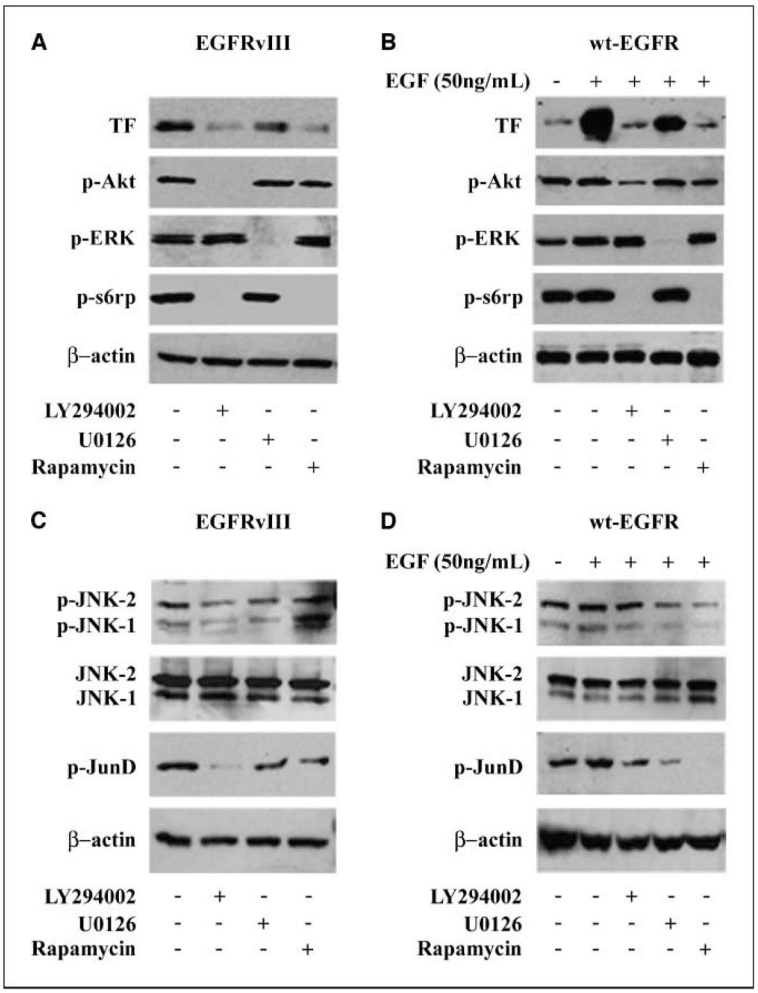

Figure 5.

EGFR-induced TF expression through AP-1 activation is signaled via the PI3K/Akt/mTOR and MAPK/ERK1/2 pathways. *A*, Western blot of cell lysates from U87MG-EGFRvIII gliomas. *B*, Western blot of cell lysates from U87MG-wt-EGFR gliomas under basal and EGF-stimulated conditions. Inhibition of PI3K (*LY294002*), MAPK/ERK1/2 (*U0126*), and mTOR (*Rapamycin*) caused reduced basal TF in U87MG-EGFRvIII (*A*) and reduced EGF-stimulated TF in U87MG-wt-EGFR gliomas (*B*). All the inhibitors were used at 10 μmol/L for 24 h. *β-actin*, loading controls. *C*, Western blot of cell lysates from U87MG-EGFRvIII gliomas shows that inhibition of PI3K (*LY294002*) and MAPK/ERK1/2 (*U0126*) reduced expression of p-JNK1/2. Inhibition of mTOR by rapamycin led to a moderate increase of p-JNK1/2. Basal p-JunD levels were reduced by all three inhibitors. *D*, Western blot of cell lysates from U87MG-wt-EGFR gliomas shows that EGF-stimulated p-JNK1/2 and p-JunD levels were attenuated by all three inhibitors. *β-actin*, loading control.

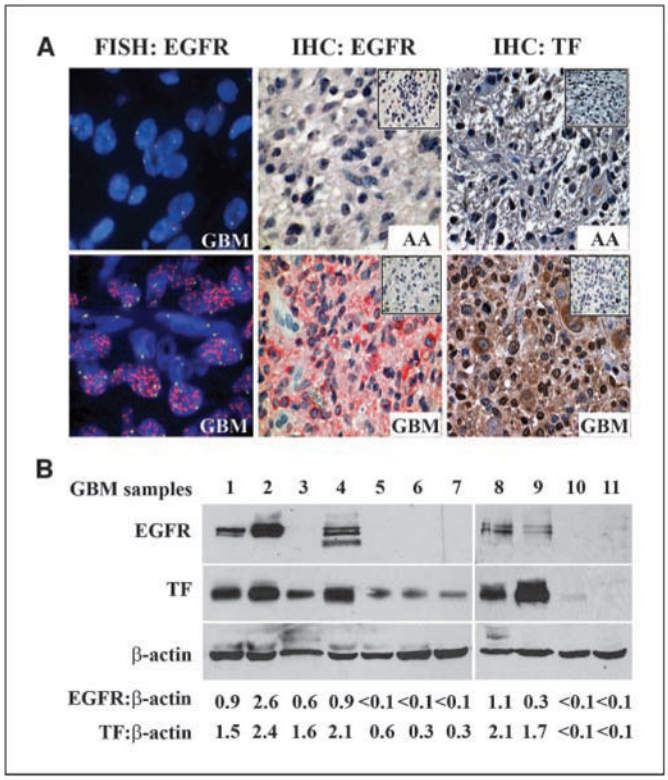

Figure 6.

Analysis of EGFR and TF expression in human AA and GBM samples. *A*, FISH analysis of *EGFR* gene status and immunohistochemical (*IHC*) analysis of EGFR and TF protein in human GBM and AA specimens. *Left*, representative fluorescence images showing the *EGFR* (*orange*) and chromosome 7 centromeric (*green*) signals in interphase GBM cells. *Left top*, GBM specimen that is nonamplified for *EGFR* shows roughly equal numbers of EGFR and centromeric signals per nuclei (typically two *EGFR* signals per nuclei). *Left bottom*, GBM with *EGFR* gene amplification shows greatly increased signals for *EGFR* compared with centromeric signal (>10 *EGFR* signals per nucleus). *Middle*, immunohistochemical analysis of EGFR protein expression in human AA and GBM specimens using Fast Red for detection. *Insets*, negative controls (without primary antibodies). *Middle top*, representative image of AA, showing a lack of EGFR staining (scored as 0 in a 0–3+ scale). *Middle bottom*, representative image of EGFR staining in GBM, showing strong cytoplasmic and cell surface immunoreactivity on neoplastic cells (3+, *red*). *Right*, immunohistochemical analysis of TF protein expression in AA and GBM specimens using DAB (*brown*) for detection. *Right top*, representative image of AA, showing weak cytoplasmic TF expression (1+, *brown*) in scattered tumor cells. *Right bottom*, GBM specimen showing strong cytoplasmic TF staining (3+, *brown*) in nearly all tumor cells. *B*, Western blot analysis of EGFR and TF protein expression in 11 human GBM samples. *Lanes 1, 2, 4, 8*, and *9*, five GBM samples with moderate to strong EGFR protein expression also showed the highest TF expression. The six other samples with lower EGFR protein expression showed modest to mild TF expression. There was a strong positive correlation between EGFR and TF protein expression in these specimens based on a comparison of the EGFR:β-actin and TF:β-actin ratios, determined following densitometry ($\rho = 0.8$, Spearman's rank test). *β-actin*, loading control.

Table 1

Immunohistochemical analysis of EGFR protein expression in human GBM and AA specimens

Score	GBM/*EGFR*$^{Amp+}$ (*n* = 9)	GBM/*EGFR*$^{Amp-}$ (*n* = 14)	AA (*n* = 7)
0	0 (0%)	7 (50%)	6 (86%)
+	0 (0%)	3 (21%)	0 (0%)
++	5 (56%)	3 (21%)	1 (14%)
+++	4 (44%)	1 (8%)	0 (0%)
P[*]			
GBM vs AA	<0.001		
GBM/*EGFR*$^{Amp+}$ vs GBM/*EGFR*$^{Amp-}$	<0.001		

NOTE: 0, no staining; +, weak staining; ++, moderate staining; +++, strong staining; *EGFR*$^{Amp+}$, *EGFR* gene amplified; *EGFR*$^{Amp-}$, *EGFR* gene nonamplified.

[*] Analyzed by one-way ANOVA based on the scores of each group.

Table 2

Immunohistochemical analysis of TF protein expression in human GBM and AA specimens

Score	GBM/$EGFR^{Amp+}$ (n = 9)	GBM/$EGFR^{Amp-}$ (n = 14)	AA (n = 7)
0	0 (0%)	1 (8%)	1 (14%)
+	1 (11%)	5 (36%)	6 (86%)
++	5 (56%)	4 (28%)	0 (0%)
+++	3 (33%)	4 (28%)	0 (0%)
P*			
GBM vs AA	0.002		
GBM/$EGFR^{Amp+}$ vs GBM/$EGFR^{Amp-}$	N.S. (P = 0.22)		

NOTE: 0, no staining; +, weak staining; ++, moderate staining; +++, strong staining; $EGFR^{Amp+}$, *EGFR* gene amplified; $EGFR^{Amp-}$, *EGFR* gene nonamplified.

Abbreviation: N.S., not significant.

* Analyzed by one-way ANOVA based on the scores of each group.